Cellulose Nanowhiskers from Moso Bamboo Residues: Extraction and Characterization

Shaoping Qian, Huanhuan Zhang, and Kuichuan Sheng *

To take full advantage of moso bamboo processing waste, bamboo cellulose nanowhiskers were isolated from bamboo residues using sulfuric acid hydrolysis. Changes in bamboo cellulose at different stages of processing, as well as the roles of acid concentrations (55 wt% and 65 wt%) and hydrolysis times (1 h to 5 h) on the characteristics of nanowhiskers were investigated by scanning electron microscopy (SEM), transmission electron microscopy (TEM), thermogravimetry-Fourier transform infrared spectroscopy analysis (TGA-FTIR), synchrotron radiation wide angle X-ray scattering (WAXS), composition analysis, and Brunauer-Emmett Teller (BET) analysis. Both rod-like and network-like nanowhiskers were observed. Alkaline pretreatment removed impurities and part of the hemicellulose. Cellulose content increased to nearly 85%, and specific surface area improved as well after bleaching. Nanowhiskers had an average length of 455 nm, diameter of 12 nm, and an aspect ratio of about 37. Cellulose I was the dominant composition in bamboo cellulose; the transformation of cellulose I_α to cellulose I_β was observed. Nanowhiskers presented greater crystallinity and crystallite size than those of cellulose without hydrolysis, but lower thermal stability. These bionanowhiskers might be used as reinforcements in nanocomposites.

Keywords: Acid hydrolysis; Bamboo residue; Cellulose; Nanowhisker; Synchrotron radiation WAXS

*Contact information: College of Biosystems Engineering and Food Science, Zhejiang University, Hangzhou 310058, China; *Corresponding author: kcsheng@zju.edu.cn*

INTRODUCTION

Due to the paucity of fossil fuel resources and the increased interest in environmental protection, cellulose, the most abundant natural, biodegradable polymer, has gained importance as a sustainable and green alternative for synthetic polymers (Fahma *et al*. 2010). Cellulosic molecules in natural fiber are a linear chain composed of chair form *β*-(1,4)-D-glucopyranose units (Missoum *et al*. 2013). In the original cellulose (also called cellulose I), there are two different crystal forms, namely, cellulose I_α and cellulose I_β. The former has a triclinic cell arrangement and is usually found in algae and bacteria cellulose, while the latter is a monoclinic allomorph that is common in plant cellulose (ramie, cotton, *etc*.). Thus, cellulose from different raw biomass shows different proportions of the crystalline types. Alkali treatment removes the non-cellulosic materials from the cellulose. This cellulose, produced by conversion of natural cellulose to a soluble cellulosic derivative and subsequent regeneration, called regenerated cellulose, also known as cellulose II, which presents better thermal stability than cellulose I (Kasyapi *et al*. 2013).

Cellulosic structure consists of an ordered crystalline region and a disordered amorphous area. Its self-assembled supramolecular structure and fibril morphology are

maintained *via* covalent of anhydroglucose, inter- and intramolecular hydrogen bonding and Van der Waals forces (Notley *et al*. 2004). The covalent interaction forces can be disrupted by protons of acid catalysis, so cellulose can be hydrolyzed by acid under certain conditions, and the products can be described using the terms microfibril, microcrystalline, nanocrystalline, or nanowhisker. Cellulose nanowhiskers (CNW), mostly used as reinforcements, are rod-like with a diameter of 2 nm to 20 nm and length of 100 nm to 2.1 μm (Dufresne 2008). CNWs have the characteristics of high crystallinity, strong hydrophilicity, and high strength *etc*., and they can be widely introduced as a toughening phase into a variety of materials, including nanocomposite materials, adhesives, electronic components, biological materials, aerogel, and textiles (Brito *et al*. 2012; Cho *et al*. 2013).

Protons of acids easily infiltrate the amorphous region and rupture the glycosidic bond by acid hydrolysis, leading to the degradation of the amorphous zone. In this degradation, cellulose crystallites are obtained. Researchers have investigated the extraction of cellulose whiskers from microorganisms and raw plant materials including ramie, coconut shell, algae, hemp, sisal, wood flour, bacteria, rice husk, jute, kraft pulp, and cotton linter (Habibi *et al*. 2010; Johar *et al*. 2012; Lu and Hsieh 2012; Ni *et al*. 2012; Rosa *et al*. 2012; Morais *et al*. 2013). However, the morphology and dimension of nanowhiskers, to a certain extent, also depend on the type of biomass used due to cellulosic structural differences such as crystallinity and amorphous area (Siqueira *et al*. 2010).

Moso bamboo (*Phyllostachys heterocycla*) is a common forest resource that grows abundantly in many tropical and subtropical regions in the world, especially in Zhejiang Province, China. It has been widely used in furniture manufacturing, construction materials, and household items for thousands of years. The abundance of uses is due to its fast growth, high strength, and surface hardness as well as easy machinability (Qian *et al*. 2015). However, a large amount of moso bamboo residues, which are derived from bamboo products processing, is underused. Bamboo contains 40% to 65% cellulose content, which is high compared with the cellulose content of wood (Yang *et al*. 2008). Thus, bamboo residue is a good source of renewable nanobiobased filler. Brito *et al*. (2012) and Lu *et al*. (2015) prepared cellulose nanocrystals from bamboo fibers by sulfuric acid and phosphoric acid, and the lengths of the nanocrystals were around 100 nm, but the characterization of nanocrystals were insufficient. Visakh *et al*. (2012a; 2012b), who employed bamboo cellulose nanowhiskers as reinforcement in rubber composites, found that the high length and aspect ratio improve the composite performance. To date, the CNW exhibits a wide utilization potential, and the extraction of CNWs from bamboo sources is reported. However, the comprehensive characterization of bamboo cellulose nanowhisker (BCNW) are insufficient. The influence of different process conditions on the isolation and composition of BCNW needs investigation.

In this paper, the effects of different concentrations of sulfuric acid treatments on bamboo particles were studied. BCNWs were prepared using two acid concentrations and different hydrolysis times. The resulting BCNWs were characterized by scanning electron microscopy (SEM), transmission electron microscopy (TEM), thermogravimetry-Fourier transform infrared spectroscopy (TGA-FTIR), composition analysis, Brunauer-Emmett Teller (BET) analysis, and special synchrotron radiation wide angle X-ray scattering (WAXS) at No. BL16B beamline of Shanghai Synchrotron Radiation Facility (SSRF). The changes of bamboo cellulose at different stages of

processing were investigated. These high length and high aspect ratio whiskers could be used as enhancements in the preparation of nanocomposites with high strength and high energy storage, which can be alternatives to fibers and carbon nanotubes.

EXPERIMENTAL

Materials

Moso bamboo residues were supplied by a local moso bamboo processing factory, Lin'an, Zhejiang Province, China. The particles were screened through a mesh size of 100 and dried at 105 °C to a constant weight before further use. The chemicals, sodium chlorite, sodium hydroxide, acetic acid, sulfuric acid, acetone, uranyl acetate, of ACS grade were used as purchased (Aladdin, Shanghai, China).

Methods

Pre-hydrolysis investigation of bamboo particles

Cellulosic structure is susceptibility to aqueous acid, and its hydrolysis is closely related to processing time, acid concentration, temperature, and bath ratio. By consulting the literature (Bondeson *et al*. 2006), a temperature of 45 °C, bath ratio of 1:8.75, and treating time of 60 min were selected for the pre-hydrolysis test. Dried bamboo particles were immersed in sulfuric acid with different concentrations of 25%, 35%, 45%, 55%, and 65% by weight and stirred for 60 min at 45 °C. The particle to solution ratio was fixed at 1:8.75. After each acid hydrolysis, the suspension remained standing for 30 min for observation of the hydrolysate. Samples and appearances are listed in Table 1.

Table 1. Pre-Hydrolyzed Bamboo Particles

Sample	Acid Concentration (wt%)	BCNW Suspension Appearance
1	25	Stratification, obvious white particles
2	35	Stratification, obvious white particles
3	45	Slight stratification, milky suspension
4	55	No stratification, milky suspension
5	65	No stratification, milky suspension
6	75	No stratification, tan solution

Preparation of bamboo cellulose nanowhiskers

Bamboo particles of 100 mesh were soaked in 4% (w/v) NaOH solution at 80 °C for 24 h, rinsed with distilled water, and dried at 105 °C. After this, most of the noncellulosic materials were removed; the remaining part was mercerized cellulose. Alkaline treated cellulose (AC) was bleached with 15% (w/v) $NaClO_2$ solution with about 20 drops of acetic acid in it at 45 °C overnight. The AC was rinsed with distilled water and dried at 105 °C. The bleaching process was repeated to get white bleached cellulose (BC). Acidolysis tests of BC were carried out with two acid concentration (55 wt% and 65 wt%) based on pre-study and varying hydrolysis time intervals of 1 h to 5 h (Table 2). After each acid hydrolysis, ice water was added to stop the reaction, and the material was transferred to a centrifuge tube. The excess sulfuric acid was removed by

centrifugation (12000 rpm for 5 min) using a PK 120 centrifuge (ALC, Winchester, UK). The supernatant was discarded, and the precipitate was again washed with deionized water and centrifuged. This process was repeated 3 times. The material was dialyzed with tap water for 3 days to remove other ionic materials (regenerated cellulose membrane, Fisher, Shanghai, China, cut off 8000-12000 Da). BCNWs were freeze-dried (5810R, Eppendorf, Hamburg, Germany) for further characterization.

Table 2. Bio-Nanowhiskers Samples

Sample	Sample Composition	Reagent Used	Reaction Temperature (°C)	Reaction Time (h)
Raw BP	Raw bamboo particles	-	-	-
AC	Regenerated cellulose/ pulp	4% NaOH	80	24
BC	Bleached pulp	15% $NaClO_2$	45	24
C51	Bleached pulp	55 wt% H_2SO_4	45	1
C52	Bleached pulp	55 wt% H_2SO_4	45	2
C53	Bleached pulp	55 wt% H_2SO_4	45	3
C54	Bleached pulp	55 wt% H_2SO_4	45	4
C55	Bleached pulp	55 wt% H_2SO_4	45	5
C61	Bleached pulp	65 wt% H_2SO_4	45	1
C62	Bleached pulp	65 wt% H_2SO_4	45	2
C63	Bleached pulp	65 wt% H_2SO_4	45	3
C64	Bleached pulp	65 wt% H_2SO_4	45	4
C65	Bleached pulp	65 wt% H_2SO_4	45	5

Scanning electron microscopy (SEM)

The surface morphology of raw BP and different treatment BCNWs were observed using field launch scanning electron microscopy (S-8010, Hitachi, Tokyo, Japan). Samples were coated with gold before observation. The launching voltage of electron microscopy was 4.0 kV.

Thermogravimetry-Fourier transform infrared spectroscopy analysis (TGA-FTIR)

A TGA Q500 thermogravimetry analyzer (TA Instruments, New Castle, DE, USA) and Nicolet 6700 Fourier infrared spectrometer (Thermofisher Scientific, Waltham, MA, USA) were used. Samples (about 15 mg) were heated from room temperature to 600 °C under N_2 atmosphere with a heating rate of 10 °C/min. The temperature of the transfer line between the TGA and FTIR equipment was 210 °C. For FTIR, the resolution was 4 cm^{-1}, and the scanning range was 4000 to 400 cm^{-1}. A total of 16 scans were collected.

Composition analysis

The cellulose, hemicellulose, and lignin content analysis of samples were carried out at Bioenergy and Biomaterials Laboratory at Zhejiang University (Zhejiang, China) with a raw fiber analyzer (FIWE-6, VELP) according to the Van Soest method (Qian *et al*. 2013). About 1.00 g of sample was used, and the content of neutral detergent fiber, acid detergent fiber, acid detergent lignin, and acid-insoluble ash was extracted by a series of solutions and solvents. Through conversion, the content of cellulose, hemicellulose, and lignin was obtained.

Specific surface area measurements

A static nitrogen absorption instrument (JW-BK, Jinghong, Beijing, China) was used to measure the specific surface area of bamboo particles and BCNWs. Ten nitrogen adsorption pressure intervals were set, and adsorption was conducted under liquid nitrogen environment at -196 °C with about 0.45 g of dried sample. The Brunauer-Emmett Teller (BET) method was adopted to calculate the specific surface area.

Synchrotron radiation WAXS

WAXS tests were performed at the BL16B beamline of Shanghai Synchrotron Radiation Facility (SSRF) (Shanghai, China). The wavelength of radiation source was 0.124 nm. The sample-to-detector distances and acquisition time were 0.11 m and 10 s, respectively. Scattering patterns were recorded by a Rayonix SX-165 CCD detector (Rayonix, Evanston, IL, USA), which had a resolution of 2048 × 2048 pixels and a pixel size of 80 × 80 μm^2. 2D data was converted into 1D data by circular averaging with a Fit2D software (European Synchrotron Radiation Facility, Grenoble, France).

Transmission electron microscopy (TEM)

A BCNW suspension with mass fraction of 0.05% was prepared and ultrasonically treated for 30 min. Drops of BCNW aqueous suspensions were deposited on copper TEM grids, and the excess of water was absorbed with a tissue. The specimens were stained with 2% uranyl acetate and observed using a JEM 1230 transmission electron microscope (JEOL, Tokyo, Japan) operating at 200 kV. The BCNW dimensions were determined with Image Tools software (UTHSCSA, San Antonio, TX, USA).

RESULTS AND DISCUSSION

Effect of Sulfuric Acid Concentrations

Diluted and concentrated acid are typically employed in natural fiber hydrolysis. Diluted acid (1 wt% to 3 wt%) hydrolysis requires high temperature, high pressure, long hydrolysis time, and high acid consumption. Thus, concentrated sulfuric acid hydrolysis was conducted in this study. When fibers were hydrolyzed to nanoscale, the appearance of the suspensions changed, and the dispersion became more homogeneous. As shown in Table 1 and Fig. 1, 25% to 45% sulfuric acid partly hydrolyzed cellulose. However, the acid concentration was too low to hydrolyze the fibers adequately. Because most of the crystalline fibers were decomposed incompletely, the suspensions separated, and microcrystallite portions precipitated. Less precipitate and more uniform dispersal of BCNWs were observed at 55 wt% and 65 wt% sulfuric acid concentrations. Cellulose begin to degrade into glucose and oligomers which are soluble when the acid concentrations are higher than 62%. At 75% sulfuric acid, there was a brown color, indicating the dehydration and carbonization of cellulose and hemicellulose. Thus, 55% and 65% solutions were used for further investigation.

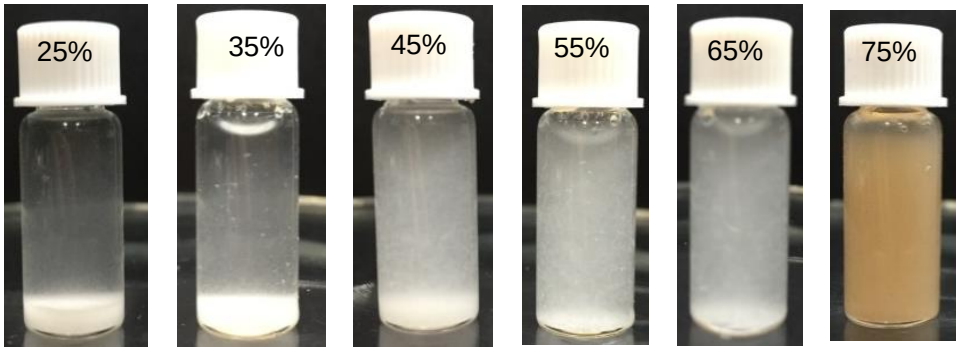

Fig. 1. Appearance of hydrolysis of bamboo particles using different concentrations of acid

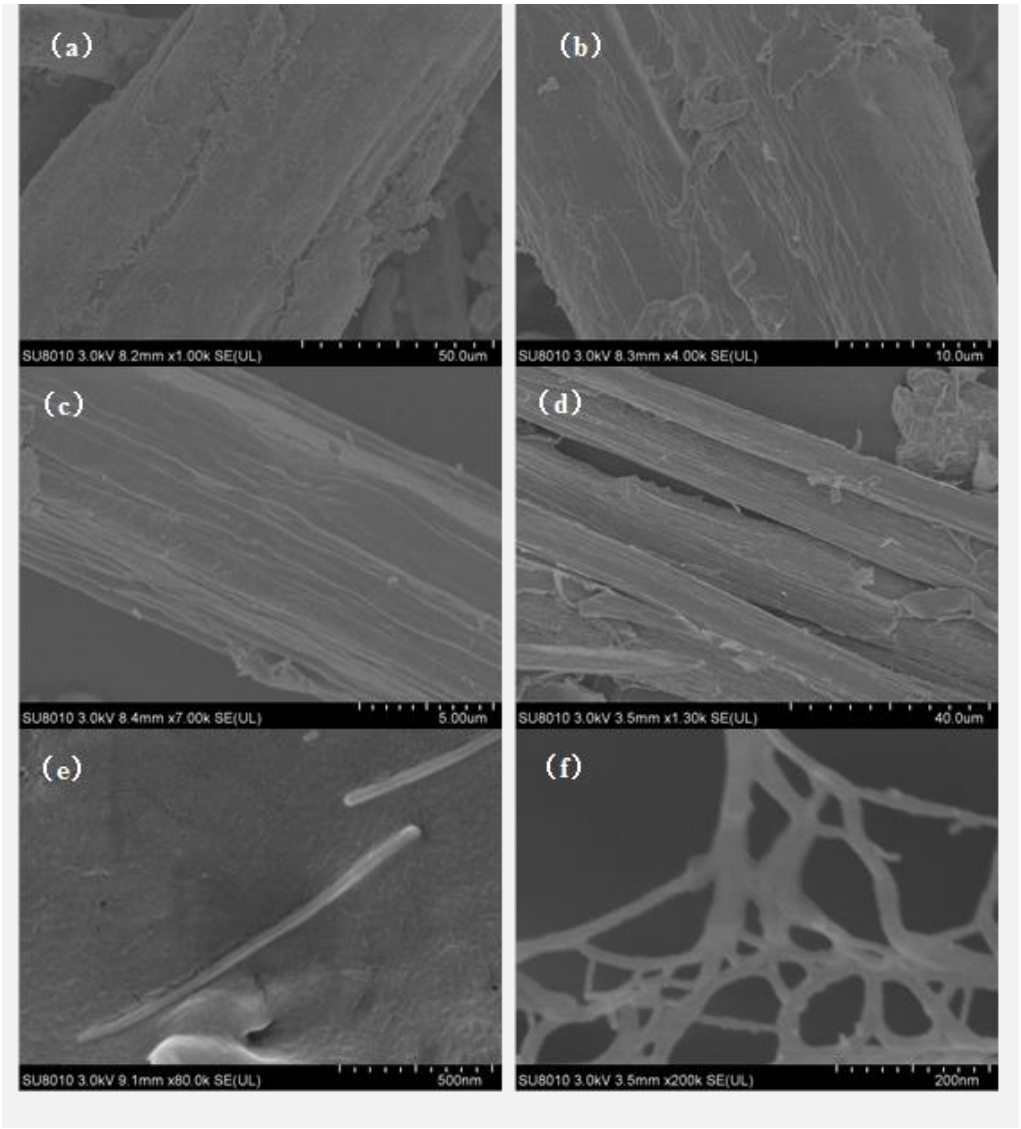

Fig. 2. SEM images of bamboo cellulose with different treatment. (a) Raw BP; (b) Alkali treated (AC); (c) Bleached (BC); (d) 65 wt% H_2SO_4 1 h (C61); (e) single BCNW (C63); (f) 65 wt% H_2SO_4 3 h (C63)

SEM Analysis

The surface microscopic characteristics of raw BP and BCNWs are shown in Fig. 2. The surface of raw bamboo particle was rough and covered with impurities, and the surface texture was rare (Fig. 2a). After alkaline treatment, lipids and inorganic impurities on the fiber surface were eliminated and gradually mercerized. Due to the partial removal of hemicellulose, fibrils of bamboo gradually appeared along with more grain (Fig. 2b). After bleaching, the overall structure of bamboo pulp was destroyed. Fibers were separated into a small dimension. Thus, a majority of lignocellulose materials gradually degraded under strong oxidization. Microfibrils of bamboo and obvious grooves were clearly seen in Fig. 2c. The influence of different acid concentration and hydrolysis time on the bamboo particles is described in Fig. 2 (d to f). Figure 2d shows the collapse of bamboo fiber, which was disintegrated into microfibrils by acidolysis, and the gaps within the fibers were clearly observed after sulfuric acid of 65 wt% treatment for 1 h. BCNWs formed by bamboo fibrils hydrolysis are illustrated in Fig. 2e and f. The diameters of BCNW were several nanometer to dozens of nanometer, the length presented hundreds of nanometer, and the length to diameter (*L*/*D*) ratio were large. BCNWs with similar appearances were obtained with 55 wt% sulfuric acid for 4 h or 65 wt% sulfuric acid for 3 h. Interestingly, rod-like shapes and network-like BCNW structures were observed, which is different from those derived from jute (Kasyapi *et al*. 2013), coconut husk (Fahma *et al*. 2010), rice husk (Rosa *et al*. 2012), and cotton (Satyamurthy *et al*. 2011). It can possibly be attributed to the fibrillation of CNW, which occurred in the nanocellulose prepared with a homogenizer. Thus, the fibrillated CNW has a higher surface area and better characteristics as a polymer matrix filler.

Composition Analysis

Changes in bamboo particles (cellulose, hemicellulose, lignin, and ash content) under different process conditions are shown in Table 3. Raw BP had a cellulose content of 64%. Thus, it has more potential to prepare cellulose nanowhiskers because its cellulose content is higher than other natural fibers such as banana (54% to 64.4%) (Cherian *et al*. 2008), bagasse (44.9% to 45%) (Cerqueira *et al*. 2007), and coconut shell (32.5% to 45.9%) (Brígida *et al*. 2010). After alkaline treatment and bleaching, the hemicellulose and lignin content in bamboo particles gradually declined. During acid and alkaline treatment, the main chemical components of hemicellulose, galactoglucomannan, and arabinogalactan dissolve into oligosaccharides and water-soluble monosaccharides. With increasing acid concentration and treatment time, the cellulose content of samples gradually increased; the highest value of 93.01% was obtained at 65 wt% acid treatment for 3 h, which was higher than that obtained from cotton linter (Morais *et al*. 2013). Lignin content decreased sharply after bleaching, which indicates that chemical bonds were destroyed and a large number of syringyl, guaiacyl, and hydroxyphenyl aromatic compounds were hydrolyzed under strong oxidation. Cellulose and hemicellulose are believed to be linked through hydrogen bonds, whereas hemicellulose and lignin are bonded with both hydrogen bond and chemical bonds such as benzyl ether linkage, phenyl glycoside linkage, hemiacetal, and acetal linkage. Most of these bonds are broken by hydronium in acidic conditions. Therefore, the integral structure of bamboo particles gradually disintegrates, and the contents of hemicellulose and lignin decrease.

Table 3. Composition Analysis of BP and BCNW with Different Treatments

Samples	Cellulose (%)	Hemicellulose (%)	Lignin (%)	Ash (%)
Raw BP	64.88	23.57	16.52	0.356
AC	72.59	17.29	12.76	0.280
BC	84.17	10.21	1.38	0.072
C51	86.50	6.21	1.21	0.069
C53	89.95	4.95	0.58	0.065
C55	87.52	4.24	0.45	0.061
C61	88.24	5.21	0.86	0.057
C63	93.01	4.32	0.47	0.065
C65	87.89	3.14	0.42	0.084

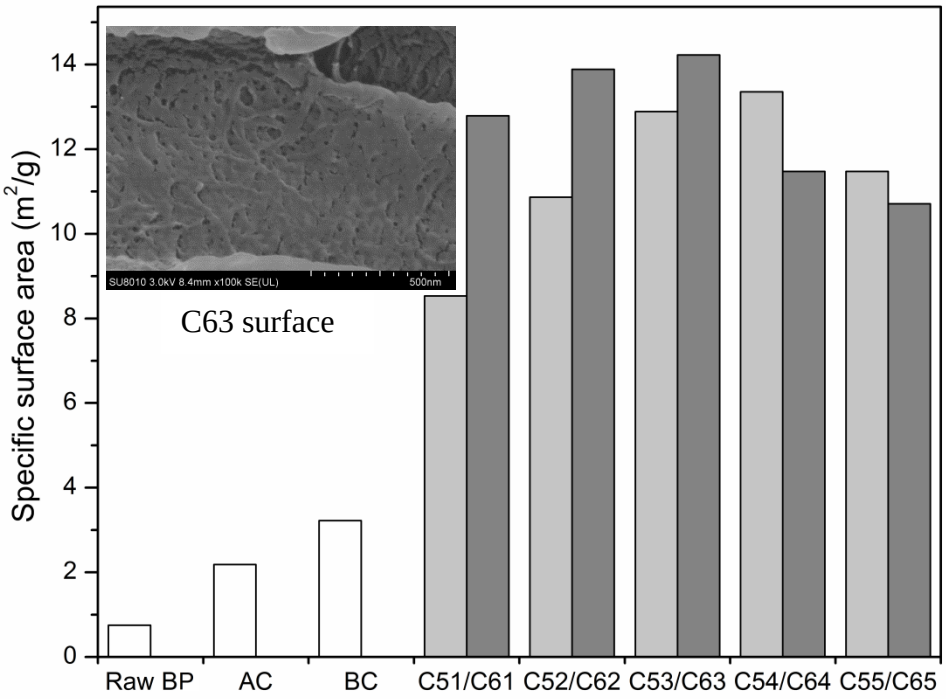

Fig. 3. Specific surface area of BP and BCNW with different treatment

Effect of Acid Hydrolysis on Specific Surface Area

The specific surface areas of raw BP and BCNWs are shown in Fig. 3. Raw BP exhibited a smaller specific surface area (0.751 m^2/g) than after alkaline treatment or bleaching. SEM observation verified that surface impurities and BP extractives were removed, which resulted in deepening of surface texture and grooves of bamboo particles. Thus, the surface pores of BP were extended and multiplied after alkaline and bleaching treatment. Bamboo fibrils, with the addition of sulfuric acid, were seperating constantly, and whiskers were eventually separated with increased treatment time. After a 65 wt% sulfuric acid treatment for 3 h, BCNW showed the maximum specific surface area of 14.225 m^2/g. After 55 wt% sulfuric acid treatment for 4 h, the specific surface area of 13.355 m^2/g was obtained. The surface of the C63 sample contained many pores. This effect may be caused by the partial ruptures of glycosidic bonds and formation of D-glucose, which dissolves in solution. The degree of cellulosic hydrolysis varied in acid concentration and processing time. More pores led to a larger specific surface area.

However, excessive treatment time dissolved the cellulose so that the specific surface areas of C64, C65, and C55 decreased.

TEM Analysis

As shown in Fig. 4a, bamboo cellulose nanowhiskers were evenly dispersed in aqueous solutions. In Fig. 4b, cellulose whiskers showed nano-aggregation morphology, closely spaced crystal morphology, and isolated single whiskers. Cellulose nanowhiskers had an rod-like appearance, and the high average length, diameter, and length to diameter ratio (L/D) were 455 nm, 12 nm, and 37, respectively. Cellulose nanowhiskers prepared from cotton linter, coconut shells, rice husk, cotton, and wood (Chen *et al*. 2010) show aggregated distribution similar to that of BCNWs, whereas the aspect ratio of BCNWs is higher than those whiskers. In addition, the observed dimensions of BCNW were different from bamboo cellulose nanocrystals with the length of 100 nm to 200 nm and a width of 15 nm to 30 nm reported by Lu *et al*. (2015). Most likely, the acid was not strong enough to break down the cellulose molocular chain at a relativly low concentration. As a result, the cellulose nanocrystal size was large. From the perspective of nanostructures, the crystallography and biosynthesis of cellulose strongly suggests that such a structure is made up of more glucose parallel chains units, with which BCNWs may preferably reinforce a polymer matrix (Siqueira *et al*. 2010).

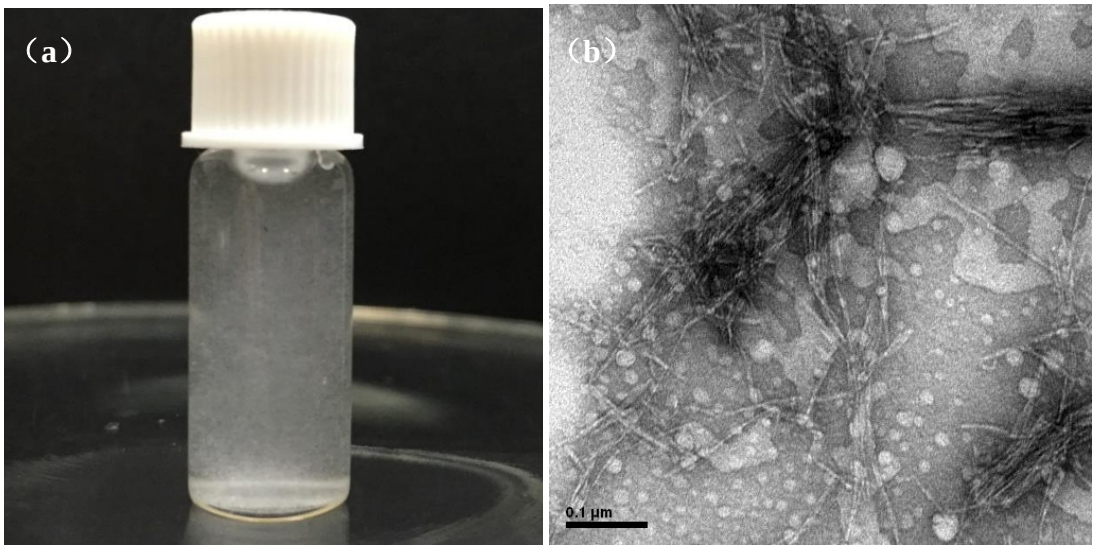

Fig. 4. Cellulose nanowhisker suspension (a) and TEM picture of C54 (b)

WAXS Analysis

Raw BP and cellulose with different treatments were analyzed by synchrotron radiation WAXS (Fig. 5). The presence of three strong peaks at 2θ = 12.5°, 17.7°, and 27.6° are the characteristics of cellulose I, corresponding to the $101, 10\bar{1}$, 200, and 040 crystallographic planes (Padzil *et al*. 2015; Indran and Raj 2015; Singh *et al*. 2015). The major peak intensity was increased and shifted, indicating an increased crystallinity index and the conversion of cellulose I_α to cellulose I_β, which is supported by Kasyapi *et al*. (2013). A small peak around peak at 12.5° showed the crystallographic plane transformation of cellulose I from $10\bar{1}$ to 101 after alkaline and bleaching treatment. After acid treatment, the diffraction peaks of 23.3° shifted to 22.1°, which was also due to transformation of cellulose I_α to cellulose I_β (Borysiak and Garbarczyk 2003). The

intensity peak of 27.6° of cellulose I also strengthened with hydrolysis. Notably, the X-ray used was a different wavelength (0.124 nm) from the traditional X-ray (0.154 nm). Though the diffraction angles were different from those previously reported (Mao *et al*. 2015), the lattice spacing calculated from the Bragg equation was the same. The average crystallite size, corresponding to plane 200, was estimated by the Debye-Scherrer equation,

$$D = \frac{k\lambda}{\beta \cos\theta} \quad (1)$$

where D refers to the average crystallite size, β presents the full width at half maxima, λ is the wavelength of the X-ray (0.124 nm), and θ is half of the angle for the corresponding peak (2θ).

Crystallite size increased from 2.4 nm (raw BP) to 4.5 nm (BC) and further increased to 6.8 nm (C63) during acid hydrolysis. However, no significant difference was noticed between BCNWs using varying acid treating times. The trend of crystallite size variation of cellulose matches well with that obtained from jute (Kasyapi *et al*. 2013).

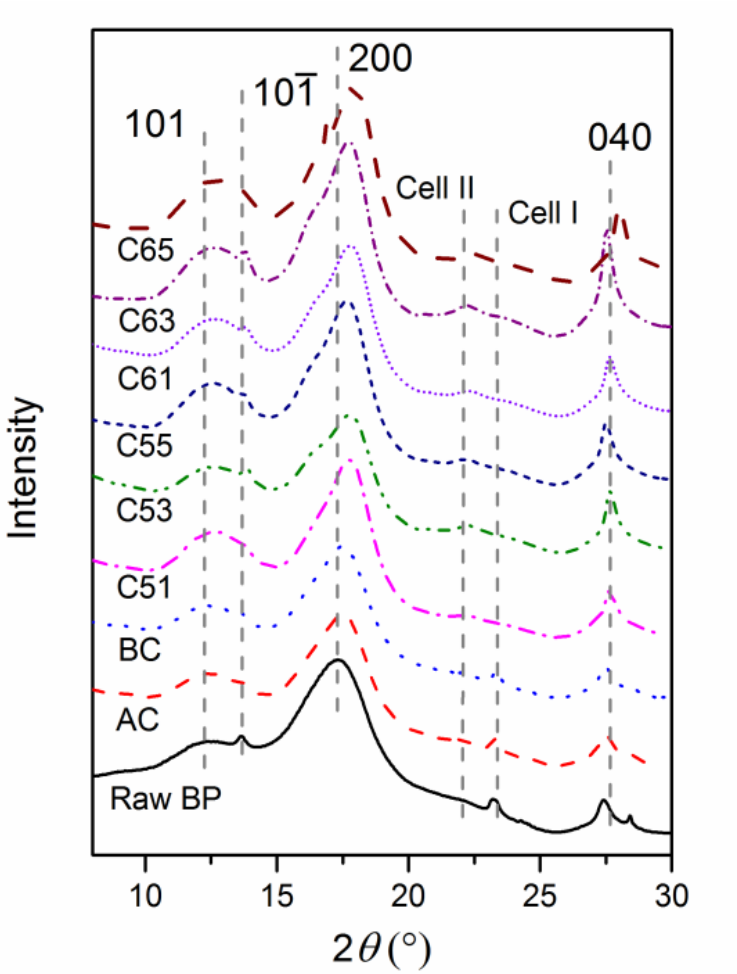

Fig. 5. WAXS patterns of raw BP, cellulose and BCNWs. Numbers denote the Miller indices of crystal lattice. The X-ray wavelength was 0.124 nm.

TGA-FTIR Analysis

Figure 6a shows the thermograms depicting TGA and DTG curves for raw BP, alkaline treatment, bleaching, and 65 wt% sulfuric acid hydrolysis for 3 h samples under nitrogen atmosphere. As revealed in DTG curve, in raw BP, a small shoulder was found at low temperature direction of degradation peak, which is similar to jute fiber. This was attributed to the presence of impurities such as lignin and hemicellulose. This shoulder was completely absent in the BC due to the removal of noncellulosic components. Hemicellulose contains a mixture of various polymerized monosaccharides (xylose, mannose, glucose, galactose, arabinose, *etc*.). With lower degree of polymerization, hemicellulose showed lower thermal stability than cellulose. The main temperature of hemicellulose degradation was from 185 °C to 325 °C, as reported (Ma *et al*. 2015).

In addition, all samples presented a single degradation peak, which is common in the pyrolysis of biomass containing lignin, such as pine and cornstalks (Ma *et al*. 2015). The onset degradation temperature of BCNW (285 °C) was lower than that of the raw BP and treated cellulose. This result suggests that the interactive force between cellulosic microfibrils and the degree of crosslinking between polysaccharide decreased after treatments, which occurred because of the decomposition of xylan, mostly in hemicellulose and the disintegration of amorphous lignin. The formation of cellulose nanocrystals led to an increase in surface area, seen in BET analysis. Thus, BCNW was susceptible to exposure to heat and facilitated thermal transfer. The maximum temperature of thermal degradation rate (T_{max}) was the same in raw BP, AC, and BC, whereas it decreased by 50 °C after hydrolysis. A decreased T_{max} was also observed in nanocellulose crystals prepared from cotton linter (Morais *et al*. 2013), coconut husk (Fahma *et al*. 2010), and sugarcane bagasse (Cerqueira *et al*. 2007). The effect is probably attributable to the insertion of sulfate groups in the glucose residues so that less activation energy is required (Morais *et al*. 2013). Moreover, the gradation temperature range of BCNW was 285 °C to 380 °C, which is quite similar to the pure cellulose degradation along with the temperature of 290 °C to 380 °C, showing the high content of cellulose (Ma *et al*. 2015).

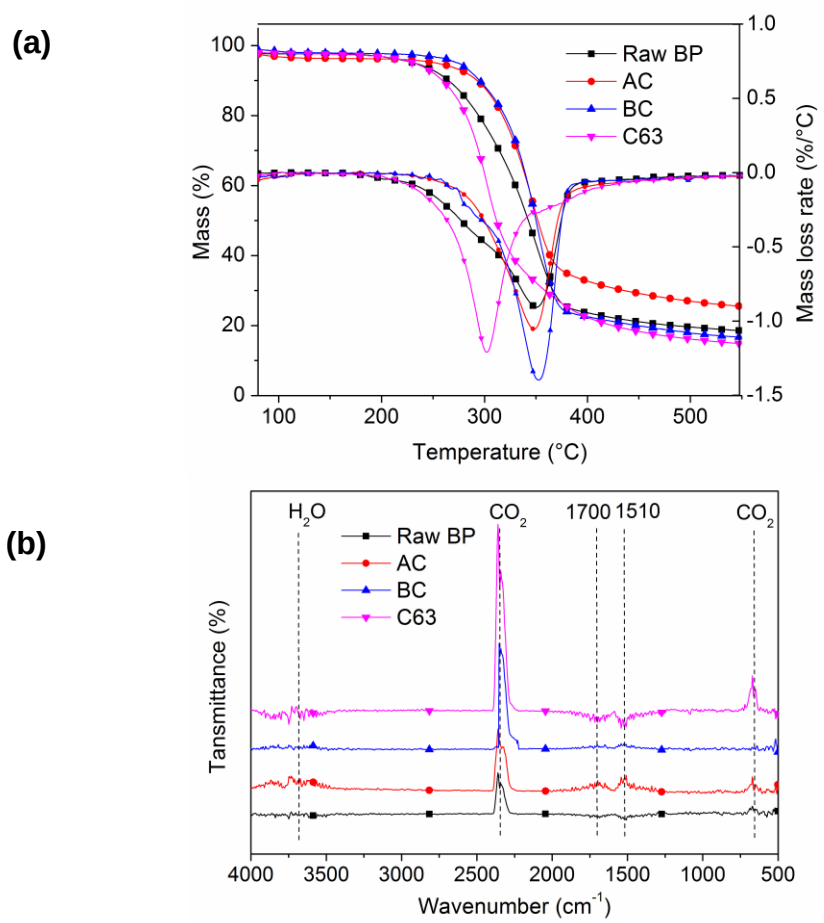

Fig. 6. (a) TGA/DTG curves and (b) FTIR spectra of raw BP and cellulose with different treatment

Degradation gas produced by the first thermal pyrolysis stage was analyzed by infrared absorption spectrum (Fig. 6b). The volatile components released from different samples varied. Strong absorption peaks located at 1700 cm^{-1} and 1451 cm^{-1} were observed in raw BP and alkaline treated BP; these peaks were attributed to aldehydes, ketones, and acids (1900 cm^{-1} to 1650 cm^{-1}) and aromatic compounds (1690 cm^{-1} to 1450 cm^{-1}) caused by the degradation of hemicellulose (Ma *et al*. 2015). Pyrolysis products of BCNW were comparatively single. CO_2 stretching and bending vibration peaks located at 2400 cm^{-1} to 2250 cm^{-1} and 586 cm^{-1} to 726 cm^{-1} suggested the high content of cellulose, and the main decomposition reactions were the decarboxylation and the fracture of carbonyl. These results also verified that alkaline treatment eliminated part of hemicellulose by mercerization, and the following bleaching process hydrolyzed most of the hemicellulose and lignin. Finally, the cellulose content greatly increased.

CONCLUSIONS

1. Bamboo cellulose nanowhiskers with a large length and aspect ratio were successfully extracted from bamboo residues using a simple method based on sulfuric acid hydrolysis. Cellulose content enormously increased to nearly 85%, and specific surface area improved as well after bleaching.

2. The surface pores and specific surface area of BCNW increased remarkably after hydrolysis. The maximum value was obtained after 65 wt% acid treated for 3 h. The rod-like BCNW had an high average length of 455 nm, diameter of 12 nm, and length to diameter ratio (*L*/*D*) of about 37. They are applicable to be used as nanofillers for reinforcement of polymer matrix.
3. The transformation of cellulose I_α to cellulose I_β was observed, and there are 4 crystallographic planes in crystallite of BCNW. The BCNW presented greater crystallinity and crystallite size than those of bamboo particles without hydrolysis. The thermal stability of BCNW was lower than that of raw BP. These findings will help to improve the knowledge on the complex characteristics of cellulose nanowhiskers.

ACKNOWLEDGMENTS

This work was financially supported by the Natural Science Foundation of Zhejiang Province (No. LY16E030003) and the National Science & Technology Pillar Program of China. (No. 2012BAC17B02). WAXS experiments were performed at the BL16B beamline of SSRF, Shanghai, China.

REFERENCES CITED

Bondeson, D., Mathew, A., and Oksman, K. (2006). "Optimization of the isolation of nanocrystals from microcrystalline cellulose by acid hydrolysis," *Cellulose* 13(2), 171-180. DOI: 10.1007/s10570-006-9061-4

Borysiak, S., and Garbarczyk, J. (2003). "Applying the WAXS method to estimate the supermolecular structure of cellulose fibres after mercerization," in: *5th International Conference on X-Ray Investigations of Polymer Structures*, Szczyrk, Poland, pp.104-106.

Brígida, A., Calado, V., Gonçalves, L., and Coelho, M. (2010). "Effect of chemical treatments on properties of green coconut fiber," *Carbohydrate Polymers* 79(4), 832-838. DOI: 10.1016/j.carbpol.2009.10.005

Brito, B. S., Pereira, F. V., Putaux, J.-L., and Jean, B. (2012). "Preparation, morphology and structure of cellulose nanocrystals from bamboo fibers," *Cellulose* 19(5), 1527-1536. DOI: 10.1007/s10570-012-9738-9

Cerqueira, D.A., Rodrigues Filho, G., and da Silva Meireles, C. (2007). "Optimization of sugarcane bagasse cellulose acetylation," *Carbohydrate Polymers* 69(3), 579-582. DOI: 10.1016/j.carbpol.2007.01.010

Chen, H., Ferrari, C., Angiuli, M., Yao, J., Raspi, C., and Bramanti, E. (2010). "Qualitative and quantitative analysis of wood samples by Fourier transform infrared spectroscopy and multivariate analysis," *Carbohydrate Polymers* 82(3), 772-778. DOI: 10.1016/j.carbpol.2010.05.052

Cherian, B. M., Pothan, L. A., Nguyen-Chung, T., Mennig, G. N., Kottaisamy, M., and Thomas, S. (2008). "A novel method for the synthesis of cellulose nanofibril whiskers from banana fibers and characterization," *Journal of Agricultural and Food Chemistry* 56(14), 5617-5627. DOI: 10.1021/jf8003674

Cho, S. Y., Park, H. H., Yun, Y. S., and Jin, H.-J. (2013). "Cellulose nanowhisker-incorporated poly(lactic acid) composites for high thermal stability," *Fibers and Polymers* 14(6), 1001-1005. DOI: 10.1007/s12221-013-1001-y

Dufresne, A. (2008). "Polysaccharide nano crystal reinforced nanocomposites," *Canadian Journal of Chemistry* 86(6), 484-494. DOI: 10.1139/v07-152

Fahma, F., Iwamoto, S., Hori, N., Iwata, T., and Takemura, A. (2010). "Effect of pre-acid-hydrolysis treatment on morphology and properties of cellulose nanowhiskers from coconut husk," *Cellulose* 18(2), 443-450. DOI: 10.1007/s10570-010-9480-0

Habibi, Y., Lucia, L. A., and Rojas, O. J. (2010). "Cellulose nanocrystals: Chemistry, self-assembly, and applications," *Chemical Reviews* 110(6), 3479-3500. DOI: 10.1021/cr900339w

Indran, S., and Raj, R. E. (2015). "Characterization of new natural cellulosic fiber from *Cissus quadrangularis* stem," *Carbohydrate Polymers* 117, 392-399. DOI: 10.1016/j.carbpol.2014.09.072

Johar, N., Ahmad, I., and Dufresne, A. (2012). "Extraction, preparation and characterization of cellulose fibres and nanocrystals from rice husk," *Industrial Crops and Products* 37(1), 93-99. DOI: 10.1016/j.indcrop.2011.12.016

Kasyapi, N., Chaudhary, V., and Bhowmick, A. K. (2013). "Bionanowhiskers from jute: Preparation and characterization," *Carbohydrate Polymers* 92(2), 1116-1123. DOI: 10.1016/j.carbpol.2012.10.021

Lu, P., and Hsieh, Y.-L. (2012). "Preparation and characterization of cellulose nanocrystals from rice straw," *Carbohydrate Polymers* 87(1), 564-573. DOI: 10.1016/j.carbpol.2011.08.022

Lu, Q., Lin, W., Tang, L., Wang, S., Chen, X., and Huang, B. (2015). "A mechanochemical approach to manufacturing bamboo cellulose nanocrystals," *Journal of Materials Science* 50(2), 611-619. DOI: 10.1007/s10853-014-8620-6

Ma, L., Zhang, Y., Cao, J. J., and Yao, J. M. (2014). "Preparation of unmodified cellulose nanocrystals from *Phyllostachys heterocycla* and their biocompatibility evaluation," *BioResources* 9(9), 210-217. DOI: 10.15376/biores.9.1.210-217

Ma, Z., Chen, D., Gu, J., Bao, B., and Zhang, Q. (2015). "Determination of pyrolysis characteristics and kinetics of palm kernel shell using TGA-FTIR and model-free integral methods," *Energy Conversion and Management* 89, 251-259. DOI: 10.1016/j.enconman.2014.09.074

Mao, H., Pan, P., Shan, G., and Bao, Y. (2015). "*In situ* formation and gelation mechanism of thermoresponsive stereocomplexed hydrogels upon mixing diblock and triblock poly(lactic acid)/poly(ethylene glycol) copolymers," *The Journal of Physical Chemistry B* 119, 6471-6480. DOI: 10.1021/acs.jpcb.5b03610

Missoum, K., Belgacem, M., and Bras, J. (2013). "Nanofibrillated cellulose surface modification: A review," *Materials* 6(3), 1745-1766. DOI: 10.3390/ma6051745

Morais, J. P., Rosa Mde, F., de Souza Filho Mde, S., Nascimento, L. D., do Nascimento, D. M., and Cassales, A. R. (2013). "Extraction and characterization of nanocellulose structures from raw cotton linter," *Carbohydrate Polymers* 91(1), 229-235. DOI: 10.1016/j.carbpol.2012.08.010

Ni, H., Zeng, S., Wu, J., Cheng, X., Luo, T., Wang, W., Zeng, W., and Chen, Y. (2012). "Cellulose nanowhiskers: Preparation, characterization and cytotoxicity evaluation," *Bio-medical Materials and Engineering* 22(1-3), 121-127. DOI: 10.3233/BME-2012-0697

Notley, S. M., Pettersson, B., and Wågberg, L. (2004). "Direct measurement of attractive van der Waals' forces between regenerated cellulose surfaces in an aqueous environment," *Journal of the American Chemical Society* 126(43), 13930-13931. DOI: 10.1021/ja045992d

Padzil, F. N. M., Zakaria, S., Chia, C. H., Jaafar, S. N. S., Kaco, H., Gan, S., and Ng, P. (2015). "Effect of acid hydrolysis on regenerated kenaf core membrane produced using aqueous alkaline-urea systems," *Carbohydrate Polymers* 124, 164-171. DOI: 10.1016/j.carbpol.2015.02.013

Qian, S., Mao, H., Sheng, K., Lu, J., Luo, Y., and Hou, C. (2013). "Effect of low-concentration alkali solution pretreatment on the properties of bamboo particles reinforced poly (lactic acid) composites," *Journal of Applied Polymer Science* 130(3), 1667-1674. DOI: 10.1002/app.39328

Qian, S., Wang, H., Zarei, E., and Sheng, K. (2015). "Effect of hydrothermal pretreatment on the properties of moso bamboo particles reinforced polyvinyl chloride composites," *Composites Part B: Engineering* 82, 23-29. DOI: 10.1016/j.compositesb.2015.08.007

Rosa, S. M. L., Rehman, N., de Miranda, M. I. G., Nachtigall, S. M. B., and Bica, C. I. D. (2012). "Chlorine-free extraction of cellulose from rice husk and whisker isolation," *Carbohydrate Polymers* 87(2), 1131-1138. DOI: 10.1016/j.carbpol.2011.08.084

Satyamurthy, P., Jain, P., Balasubramanya, R. H., and Vigneshwaran, N. (2011). "Preparation and characterization of cellulose nanowhiskers from cotton fibres by controlled microbial hydrolysis," *Carbohydrate Polymers* 83(1), 122-129. DOI: 10.1016/j.carbpol.2010.07.029

Singh, K., Sinha, T. J. M., and Srivastava, S. (2015). "Functionalized nanocrystalline cellulose: Smart biosorbent for decontamination of arsenic," *International Journal of Mineral Processing* 139, 51-63. DOI: 10.1016/j.minpro.2015.04.014

Siqueira, G., Bras, J., and Dufresne, A. (2010). "Cellulosic bionanocomposites: A review of preparation, properties and applications," *Polymers* 2(4), 728-765. DOI: 10.3390/polym2040728

Visakh, P., Thomas, S., Oksman, K., and Mathew, A. P. (2012a). "Cellulose nanofibres and cellulose nanowhiskers based natural rubber composites: Diffusion, sorption, and permeation of aromatic organic solvents," *Journal of Applied Polymer Science* 124(2), 1614-1623. DOI: 10.1002/app.35176

Visakh, P., Thomas, S., Oksman, K., and Mathew, A. P. (2012b). "Crosslinked natural rubber nanocomposites reinforced with cellulose whiskers isolated from bamboo waste: Processing and mechanical/thermal properties," *Composites Part A: Applied Science and Manufacturing* 43(4), 735-741. DOI: 10.1016/j.compositesa.2011.12.015

Yang, Z., Xu, S., Ma, X., and Wang, S. (2008). "Characterization and acetylation behavior of bamboo pulp," *Wood Science and Technology* 42(8), 621-632. DOI: 10.1007/s00226-008-0194-5

Article submitted: July 20, 2016; Peer review completed: October 2, 2016; Revised version received and accepted: November 13, 2016; Published: November 21, 2016.
DOI: 10.15376/biores.12.1.419-433